

Original Research Article

Study of Discharge Outlines of Subthalamic Nucleus-Globus Pallidus External and the Favorable Impact of Deep Brain Stimulation in the Parkinson State

Abstract:

Aims: The aim of our model is to simulate deep brain stimulation mathematically instead of doing it experimentally to check whether the outlines in Parkinson's disease helps in reducing the motor symptoms or not. The model is simulated here mathematically because clinical research is not feasible. My model is STN-GPe in which there are different differential equations. Also, to prove that the symptoms for Parkinson's disease are reduced up to 99.59%.

Study design: Cross-correlation function.

Place and duration of study: Study was conducted in private college of Gurugram from January 2021 to September 2021.

Methodology: Self designed, the conduct of the model has been accessible with the support of activity outlines produced in a normal state and Parkinson's state. These outlines have been related by finding out their correlation coefficient for dissimilar values of essential parameters. Here, a single-compartment conductance-based model is taken that concentrates on the subthalamic nucleus and synaptic input from globus pallidus (external). Current model displays extremely nonlinear behavior regarding many essential parameters.

Results: Outcomes show that the activity outlines are extremely penetrating to several essential parameters. Deep brain stimulation is measured as a harmless and well-borne surgical technique to lighten Parkinson's disease and extra movement ailments indications across some psychiatric situations. So, the deep brain stimulation technique has been applied here mathematically to find the cross-correlation between the two states. With the help of this stimulation, some promising results are obtained.

Conclusion: The conclusion is that DBS is operative at reducing motor indications of parkinsonism by 99.59%.

Keywords: Parkinson's disease, Deep brain stimulation, Movement disorder, Dopamine, Cross-correlation, Subthalamic nucleus, Basal ganglia, Parkinson's state

1. Introduction:

Parkinson's disease (PD) is considered as declining of dopaminergic neurons in the substantia nigra pars compacta (SNc) resulting in motor indications [1]. High-frequency deep brain stimulation (DBS) of the sub-thalamic nucleus (STN) or globus pallidus internus (GPi) is a recognized medical treatment to reduce the motor indications of the disorder [2,3]. This work chooses to study STN and GP because there are two main targets in Parkinson's disease patients i.e., subthalamic nucleus and globus pallidus [4,5]. Subthalamic nucleus neurons obtain glutamatergic involvements from added brain parts, counting cortical contributions via

the so-called hyper-direct trail, presenting a substitute foundation for the variation of subthalamic nucleus action [6]. As the disorder grows, the quantity of dopamine shaped in the brain declines, resulting in an individual generally being incapable to manage movement [7]. The reason for the reduction of dopamine is not well known, and hence there is currently no analysis and treatment at the initial phase [8,9]. There are various treatments at the future phases of illnesses, for example, medication and operation, to achieve its indications. Brain-related illnesses are among the utmost confusing of all the illnesses, and our unawareness of the fundamental illness device is the main problem to the expansion of improved analytical organizations [10]. Parkinson's disease changes the information designs in movement-associated pathways in the brain. Experimental outcomes executed on rats display that the activity outlines transform from single spike activity to diverse burst manner in Parkinson's disease. However, the reason for this variation in the activity outline is not so far understood. The subthalamic nucleus is the chief nuclei tangled in the basis of motor dysfunction in Parkinson's disease.

It is not identified whether DBS turns to improve or overturn neuronal movement inside a specified erection, which parts and which nerve cells inside these extents remain represented upon by DBS [11,12]. The main area tangled in the dysfunction of the brain is the basal ganglia (BG), where nuclei, SNc, striatum, STN, and GP are the main nuclei [13]. The “basal ganglia” model states to a collection of subcortical nuclei accountable mainly for motor control, besides extra roles for example motor learning, executive functions and behaviors, and reactions [14]. The external globus pallidus is the section of the globus pallidus that is comparatively away from the midline of the brain. It is occasionally used as a goal for deep brain stimulation as a treatment for Parkinson's disease. The striatum obtains contribution straight from the cortex, and also brings neurotransmitter that is blocking to the GP by different trails, direct and indirect. It has been recognized by investigators that there is an essential derivation of disorder. Currently, STN is thought to be most complicated to exhibit Parkinson's indications, but the localization to the beginning is still not clear [15]. A classical basal ganglia model has been shown in Figure 1. In this model, the focus is on the system of the STN besides globus pallidus external (GPe). Arrows having \rightarrow signs specify inhibitory synaptic networks also involvements take place from GPe to STN, GPe to GPi, GPi to the thalamus, and striatal input to GPe, while excitatory synaptic connections and inputs occur from STN to GPe, STN to GPi, excitatory input to thalamus and DBS to STN [11]. Networks remain disturbed within different nuclei in PD [16].

The basal ganglia circuits don't yield shake fluctuations in normal basal ganglia circuits. On the opposing, the tremor fluctuations linked movement is seen in STN in disorder state. The above studies recommend that STN might be measured as the goal area to inspect the motor signs and the source of PD. Hence, the activity outlines produced in the STN model are examined and associated with the behavior of the STN model in a normal state and Parkinson's disease state to discover the changing aspects of the STN-GPe loop subjected to numerous currents. A mathematical model along with primary approaches is described in section 2. Section 3 describes the susceptibility grounded learning of the model for many currents and their consequences. The implementation of DBS to the STN model is shown in section 4. Section 5 is the discussion and section 6 is the inference of the effort.

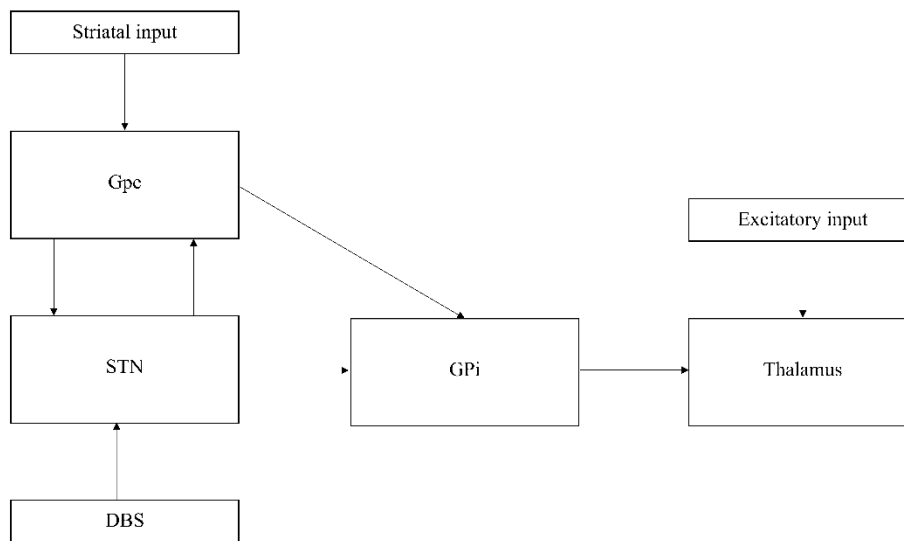


Figure 1 Structures included inside the model system.

2. Mathematical model and methods:

A dynamical model BG thalamocortical system has been proposed to achieve analytically authenticated information of electrophysiology besides the structure of the system [17]. The characteristically recognized indications are automatic actions counting shock, chorea, ballism, athetosis, and dystonia; muscular inflexibility; hypotonia; disorders in upright symmetry; walking; talking; and akinesia. Numerous theories have been estimated, suggesting that more than one mechanism is probably accountable for the therapeutic advantage [18]. Improved correlations in GPi productions and the results are assumed to be cooperative relay reliability. The efficiency of DBS is because of the replacement of compulsive GPi firing outlines with extra steady movement [19]. Each neuron is demonstrated through a similar essential set of Hodgkin–Huxley type equations [20].

To the observer the behavior of activity outlines STN- GPe system in PD and normal state, mathematical model, conductance, and time scales are used from [21]. Examination and simulated work of the STN-GPe network is achieved using MATLAB 2020a utilizing ODE45 for a time in the range of 0 to 500 ms for the extra parameters under observation. Results are simulated for both times in the range 0-500 ms and 0-1000 ms. Since the results were the same, so 0-500 ms results are shown. The objective of this examination is to offer visions into the main reasons for the sensitivity of the model in PD. The model from equation 1, contains a single leak current (I_L), reckless spike creating potassium (I_K) also sodium currents (I_{Na}), low-slung threshold T-type (I_T) also high-threshold Ca^{2+} currents (I_{Ca}), triggered Ca^{2+} voltage autonomous after-hyperpolarization K^+ current (I_{ahp}), synaptic current (I_{syn}) and applied current (I_{app}), to facilitate the equation leading the membrane potential V [22]:

$$C \frac{dV}{dt} = -I_L - I_K - I_{Na} - I_T - I_{Ca} - I_{ahp} - I_{syn} + I_{app}, \quad (1)$$

Where various membrane current is given by [12].

$$I_L = g_L \cdot (V - V_L), \quad (2)$$

$$I_K = g_K \cdot n^4 \cdot (V - V_K), \quad (3)$$

$$I_{Na} = g_{Na} \cdot m^3 \cdot (V) \cdot h \cdot (V - V_{Na}) \quad (4)$$

$$I_T = g_T \cdot a_{\infty}^3 \cdot (V) \cdot r \cdot (V - V_{Ca}) \quad (5)$$

$$I_{Ca} = g_{Ca} \cdot s_{\infty}^2 \cdot (V) \cdot (V - V_{Ca}) \quad (6)$$

$$I_{AHP} = g_{AHP} \cdot \left(\frac{(Ca)}{(Ca)+k_1} \right) \cdot (V - V_K) \quad (7)$$

Where C is the membrane capacitance, g_L , g_K , g_{Na} , g_T , g_{Ca} and g_{ahp} are the leak, potassium, sodium, high-threshold, calcium, and afterhyperpolarization conductance per unit area. V_L , V_K , V_{Na} and V_{Ca} are the leak, potassium, sodium, and calcium reversal potentials. n , m , and h are dimensionless measures among 0 and 1 that are related to potassium channel activation, sodium channel activation, and sodium channel inactivation, respectively. K_1 is the dissociation persistent of calcium-based hyperpolarizing current. To regulate the membrane resting potential through the experimental data, the applied current is used [23].

An equation that describes calcium current:

$$d \frac{[Ca]}{dt} = \varepsilon (-I_{Ca} - I_T - kCa(Ca)) \quad (8)$$

Calcium influx is categorized by ε also calcium pump rate is described by kCa . The gating variable equation for m , n , h , s , and a is described by:

$$\frac{dx}{dt} = \phi_x \left(\frac{(x_{\infty}(V) - x)}{\tau_x(V)} \right) \quad (9)$$

For the gating variable, the constant is defined by ϕ . τ_x is the time constant function. It is described by:

$$\tau_x(V) = \tau_x^0 + \tau_x^1 / \left(1 + \exp\left(-\frac{(V - \theta_x^t)}{\sigma_x^t}\right) \right) \quad (10)$$

Here, τ is the constant function and θ is the half inactivation/activation variable. The total of synaptic currents as of the GPe in addition to further nearby neurons is equivalent to synaptic current in the STN [21]. From GPe to STN synaptic inputs and feedback neurons from STN is well-defined for synaptic current I_{syn} .

$$I_{syn} = g_{g \rightarrow s} \cdot s_g (V - V_{g \rightarrow s}) + g_{f \rightarrow s} \cdot s_f (V - V_{f \rightarrow s}) \quad (11)$$

Synaptic conductance is defined by $g_{g \rightarrow s}$ and $g_{f \rightarrow s}$. Synaptic variables are defined by s_g and s_f . To display the disintegration of dopamine, synaptic inputs show the main part. The synaptic current input strength is modified in the range [22]. Lower values correlate to reduced dopamine points and higher conductance signifies the better dopamine points. The first-order kinetic equation is used for entire synaptic variables in the model course.

$$\frac{ds}{dt} = \alpha \cdot H_{\infty}(V_{presyn} - \theta_g) \cdot (1 - s) - \beta \cdot s \quad (12)$$

In which $H_{\infty}(V)$ is a sigmoid function and V_{presyn} is the synaptic potential since nearby neurons. α is alpha, θ_g is the half activation or inactivation voltage for gating variable g . The standards of synaptic variables are taken from Table 1.

$$H_{\infty}(V) = 1/[1 + \exp(-\frac{(V-\theta_g^H)}{\sigma_g^H})] \quad (13)$$

Table 1 Parameters for synapses and applied current used in our mathematical model

Synapses	Parameters
$I_{STN \rightarrow GPe}$	$g_{syn}=0.15$ and $E_{syn} = 0$
$I_{STN \rightarrow GPi}$	$g_{syn}=0.15$ and $E_{syn} = 0$
$I_{GPe \rightarrow STN}$	$g_{syn}=0.5$ and $E_{syn} = -85$
$I_{GPe \rightarrow GPe}$	$g_{syn}=0.5$ and $E_{syn} = -85$
$I_{GPe \rightarrow GPi}$	$g_{syn}=0.5$ and $E_{syn} = -85$
$I_{GPi \rightarrow TH}$	$g_{syn}=0.17$ and $E_{syn} = -85$
I_{app} (STN)	33 (HS)/ 23(PD)
I_{app} (GPe)	20 (HS)/ 7(PD)
I_{app} (GPi)	21 (HS)/ 15(PD)

3. Study of neurophysiology properties

This unit grants the study of the electrophysiological possessions of the STN-GPe neurons inside the STN neuron. The STN remains a significant assembly in the practical association of the basal ganglia [24]. A single-compartment conductance-based classical is used to signify every neuron in the STN and GPe. Eight cells of every type are advanced for the replications labeled in current learning [25]. Every neuron model involves a single set of regular differential equivalences, equals to a whole of 150 attached non-linear equivalences for the whole model. Above 100 parameter standards are desired to entirely stipulate involved differential equivalences [26]. The outlines produced for the subthalamic nucleus in a normal state are named STNHS and those produced for Parkinson's state are named STNPS. Assessment among STNHS and STNPS is achieved by cross-correlation coefficient (CCF) among these two. CCF is the degree of resemblance of two series as per a function of one relative to the second. The correlation coefficient can be calculated with the assistance of subsequent formula:

$$Correl(X, Y) = \frac{\sum(x - \bar{x})(y - \bar{y})}{\sqrt{\sum(x - \bar{x})^2 \sum(y - \bar{y})^2}} \quad (14)$$

The assessment among STNHS and STNPS has been accomplished for numerous ionic and synaptic currents, for analyzing and calculating the sensitivity of the STN model. The DBS is implemented on the STN model to study its effect on the model. All the discharge outlines in the paper are produced using equation 1. These discharge outlines are then replicated for particular ionic currents. The outcomes for parameters that are extremely penetrating for the model are exhibited. Applied current I_{app} , feedback membrane potential V_{fs} and presynaptic potential V_{presyn} are the parameters. The discharge outlines show sensitivity trade-offs as compared to the discharge outlines gained from, are accessible in the following segments. All the outputs of the figures are concerning the function of time. Thorough susceptibility study and outcomes are specified in the following segments. Through simulating the overhead model, constraints are being used as specified inside [21].

4. Results:

4.1 Sensitivity investigation for applied current

Activity outlines exhibited inside the STN-GP network in basal ganglia are classically unequal and are interrelated through the activity inside the cells. The activity outlines concerning applied current I_{app} are analyzed here. The initial reference value of I_{app} for STN in the case of normal is $33 \mu\text{A}/\text{cm}^2$ and in the case of Parkinson's is $23 \mu\text{A}/\text{cm}^2$ are taken from [27]. The value of I_{app} in the range of 23 to $33 \mu\text{A}/\text{cm}^2$ are speckled, to analyze the sensitivity of these outlines in contradiction to the applied current I_{app} [13]. These outlines reveal the sensitivity for I_{app} for together subthalamic nucleus for the normal state (STNHS) and subthalamic nucleus for Parkinson's state (STNPS). The original discharge outline for I_{app} in the original state are shown by Figure 2 for normal state and Parkinson's disease state. The values for the normal state is at $I_{app} = 33 \mu\text{A}/\text{cm}^2$ and for PD state is at $I_{app} = 23 \mu\text{A}/\text{cm}^2$. Here, the cross-correlation coefficient value is 0.958 between the two-time series.

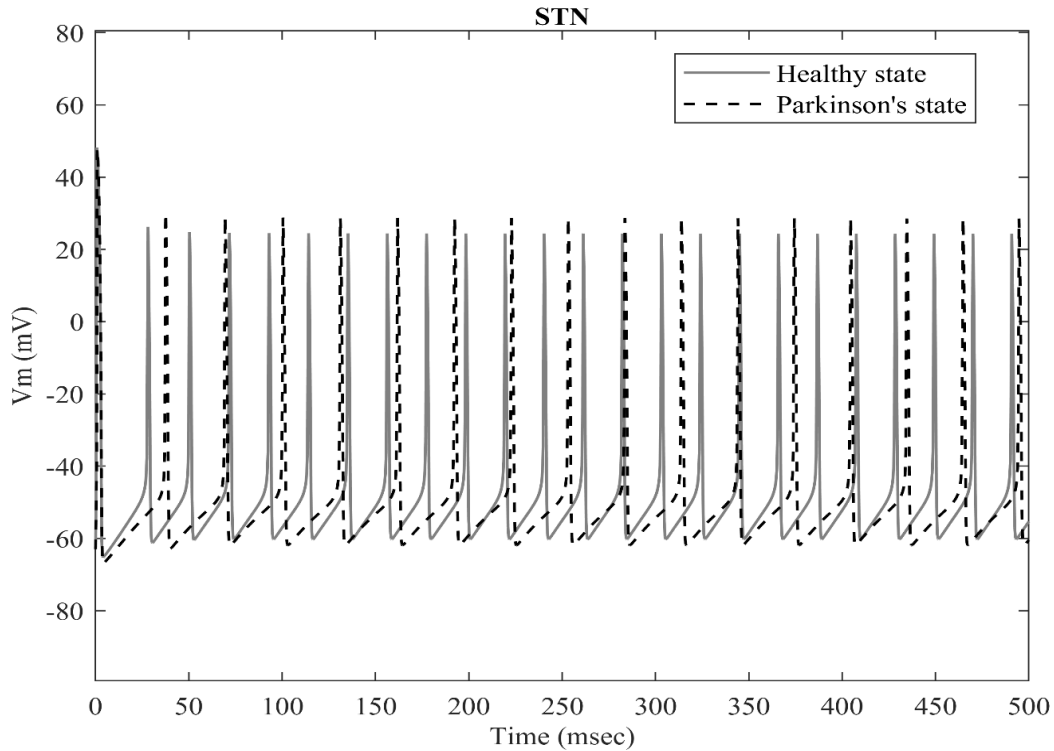


Figure 2 Variation of healthy state and Parkinson's state in STN-GPe Prototype.

The slight alteration for the value of applied current demonstrates a trade-off inside the correlation coefficient of STNHS and STNPS calculated as shown in Figure 3 which signifies the role of applied current in Parkinson's state. The maximum correlation is obtained for STNHS and STNPS is 0.8026 at $23 \mu\text{A}/\text{cm}^2$, which shows that the error margin has reduced by 80%. The graph is plotted for CCF for different values of applied current. This represents that the applied current does not play a vibrant role in reducing the symptoms of Parkinson's disease person. Increasing the value of I_{app} steadily from 23 to $33 \mu\text{A}/\text{cm}^2$ does not enhance the correlation coefficient among the two-time sequences of STN in normal state and STN in Parkinson's state. The minimum cross-correlation function is 74 for the value of applied current $33 \mu\text{A}/\text{cm}^2$ while the maximum cross-correlation function is counted as 80 which is for the value of applied current $23 \mu\text{A}/\text{cm}^2$. The applied current $31 \mu\text{A}/\text{cm}^2$, $29 \mu\text{A}/\text{cm}^2$, $27 \mu\text{A}/\text{cm}^2$ and $25 \mu\text{A}/\text{cm}^2$ are considered in between the above-mentioned range. This means that applied current shows a less effective or negligible impact in the analysis of the two-time series for the subthalamic nucleus in a normal state and Parkinson's state. Similar result has been reported in the earlier studies [15].

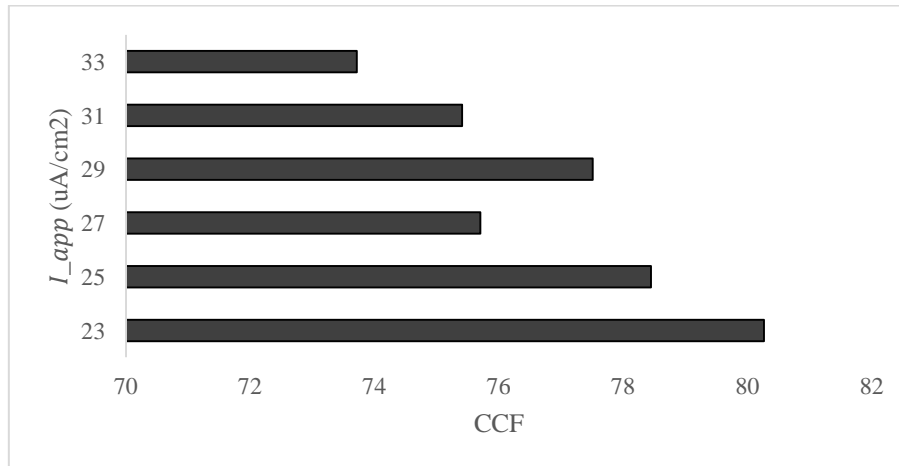


Figure 3 Variation of applied current concerning cross-correlation function.

4.2 Sensitivity investigation for pre-synaptic membrane potential

V_{presyn} is the membrane potential of a single pre-synaptic neuron. The consequence of V_{presyn} on synaptic variables has been examined which eventually disturb the STN model in normal and Parkinson's disease state. 31 mV is the orientation value considered for V_{presyn} referred by [21]. The values for $V_{presyn} = 30.5$ mV and $V_{presyn} = 31.5$ mV are taken from the research paper [13]. The pre-synaptic potential might rise or fall depending upon the networks among neighboring neurons. If the networks are disturbed, the discharge patterns might fall and if the networks are sturdy, the discharge patterns might rise [28]. Hence, it has been analyzed for disrupted and strong connections. Alteration in the pre-synaptic value does not disturb the correlation coefficient for the STN model in normal and Parkinson's disease states. Movement outlines have been displayed for both $V_{presyn} = 30.5$ mV and $V_{presyn} = 31.5$ mV in Figure 4 and Figure 5 for both normal and Parkinson's state.

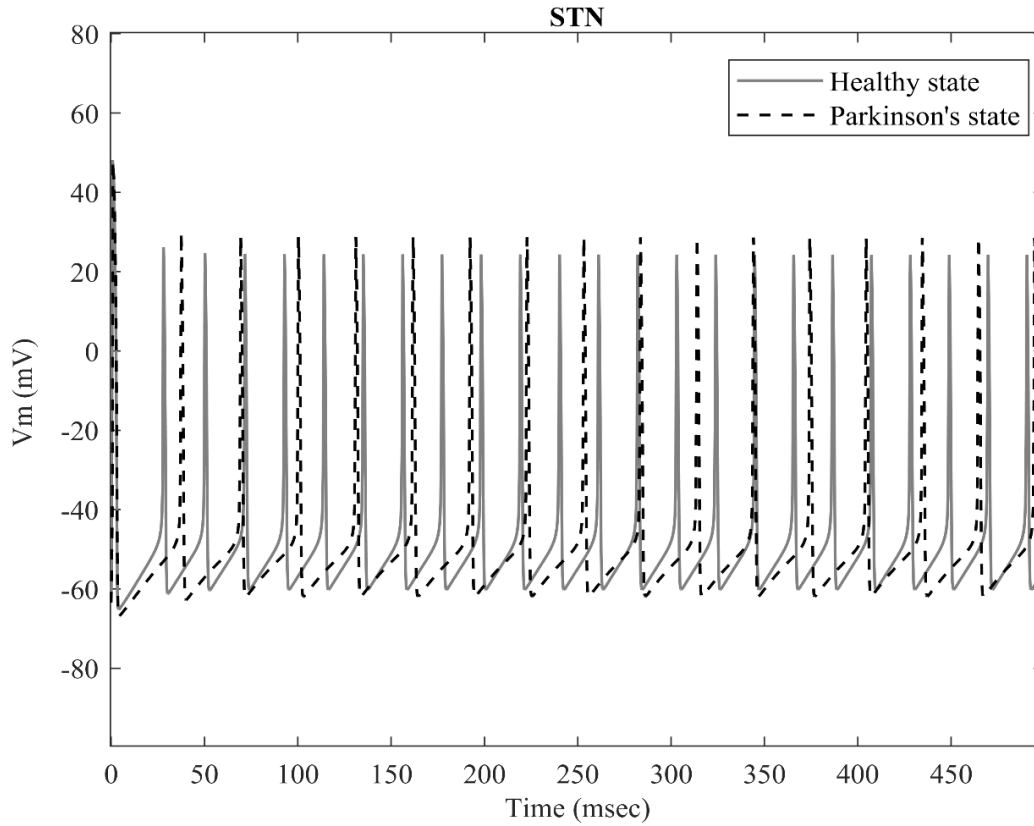


Figure 4 Variations in membrane potential concerning time for healthy state and Parkinson's state at $V_{presyn} = 30.5$ mV.

Results indicate that with the increase or decrease in the value of V_{presyn} for 30.5 mV and 31.5 mV, the correlation coefficient among the two-time sequences of STNHS and STNPS remain unchanged [13]. Table 2 displays non-linearity in dissimilar values of correlation coefficient when comparison has been made between them with activity outlines presenting linear behavior. For lag = 0, correlation coefficient is extreme in $V_{presyn} = 31$ mV. It is detected that in the STN model there is a time lag in activity outlined in normal and PD states. This data discloses a linear shift among STNHS and STNPS and the reason is not yet known. The cross-correlation among the two-time series is 9.32% in figure 4. The cross-correlation between the two-time series is 9.44% in figure 5.

Table 2 Cross-correlation coefficients for V_{presyn}

Lag	30.5 mV	31 mV	31.5 mV
0	0.093219	0.77309	0.094418
1	0.103092	0.650574	0.085267
2	0.114901	0.645038	0.083979
3	0.099946	0.649675	0.083724

4	0.118812	0.659661	0.086231
5	0.125096	0.649797	0.086154
6	0.123851	0.638336	0.085552

4.3 Sensitivity scrutiny for feedback membrane potential V_{fs}

In this sub-section, by changing feedback membrane potential V_{fs} , the outcomes of the STN model have been considered. However, the learning of this model grants the existence of oscillations when the STN-GPe loop grows stronger. This phenomenon remains strong concerning differences of numerous parameters which are dopamine-dependent. It also remains vigorous for delays in the feedback loop. The model is not steady for numerous values of V_{fs} [21]. This has been revealed in Figure 6.

The CCF is highest for the value of $V_{fs} = 14$ mV. Figure 6 displays that the correlation coefficient decreases for the values 0-2 mV, 4-6 mV, and 8-10 mV. Increases for the values 2-4 mV, 6-18 mV, and decreases at point 20 mV. This shows that the feedback membrane potential V_{fs} does not enhance the correlation coefficient among the two-time sequences of STNHS also STNPS.

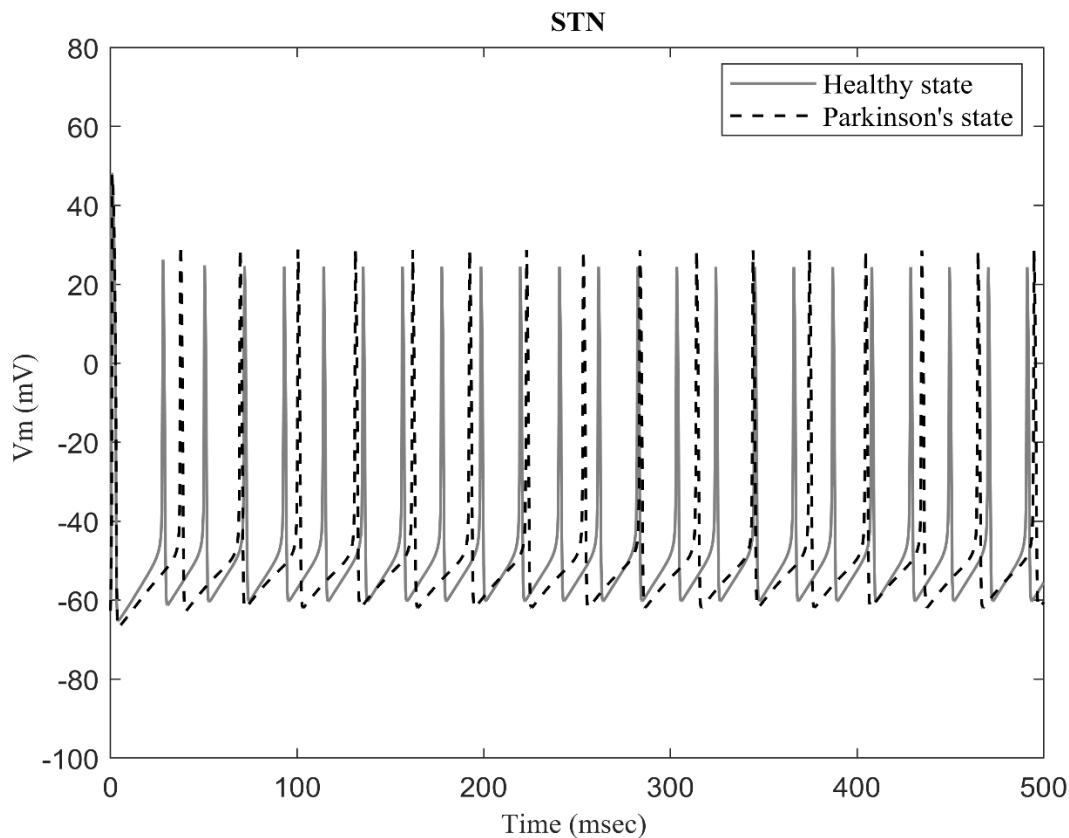


Figure 5 Variations in membrane potential concerning time for healthy state and Parkinson's state at $V_{presyn} = 31.5$ mV.

4.4 Application of DBS on the STN model

Rhythmic pulsatile voltage transients are characteristically practical to the subthalamic nucleus of the basal ganglia, throughout high-frequency DBS treatment for PD. Probably, DBS involvements that fluctuate in procedure from a high-frequency, episodic outline can be extra necessary for realizing medical purposes [29]. The DBS of STN neurons is simulated.

DBS of the STN is presented by the following model:

$$I_{DBS} = i_D \cdot H(\sin(2\pi t/\rho_D)) \cdot (1 - H(\sin \frac{2\pi(t+\delta_D)}{\rho_D})) \quad (15)$$

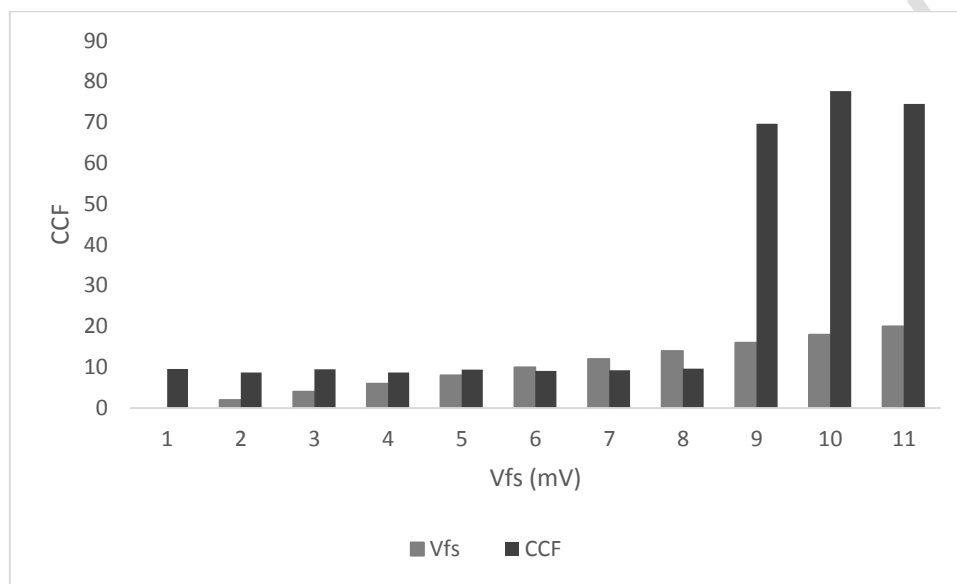


Figure 6 The relation for normal state and Parkinson's disease state in the range of $V_{fs} = 0$ -16 mV.

Where i_D resembles stimulation amplitude, ρ_D to the stimulation period, and δ_D to the period of each impulse. Also, $i_D = 200$, $\rho_D = 6$ msec, and $\delta_D = 0.6$ msec [11]. DBS offers a high frequency, excitatory contribution to STN neurons. It is discovered that this inputs centrals to the augmented action of STN neurons that sequentially stimulate GPi cells, persuading them to fire cordially at high frequency. The CCF for normal state vs Parkinson's state is 9.58%. The CCF for normal state vs Parkinson's state when DBS is applied is 99.59% as shown in Fig. 7. Since the maximum cross-correlation coefficient is 1 and the result obtained is 0.9959 when DBS is applied to Parkinson's state. It shows that the results obtained are promising because it reduces symptoms of Parkinson's state.

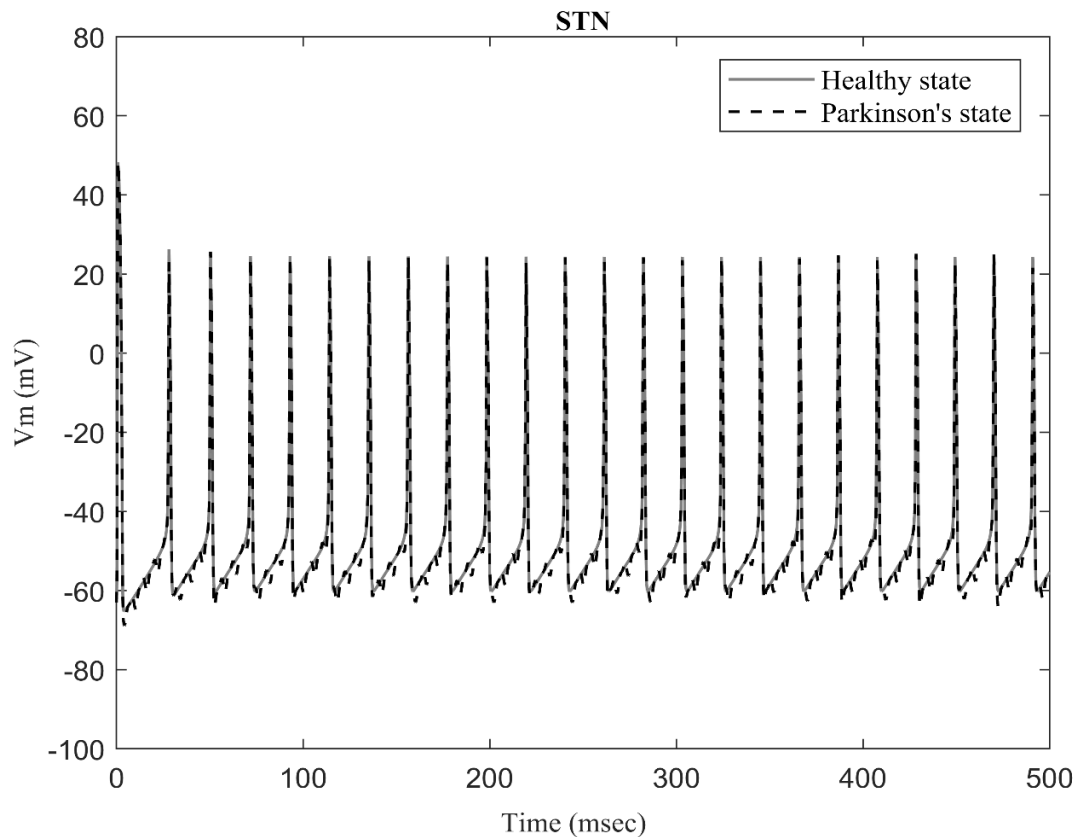


Figure 7 Discharge patterns produced in STNHS and STNPD after application of DBS where Parkinson's state has reached the healthy state.

5. Discussion:

Ejection outlines of the single-compartment model have been examined in the hunt for discovering the constraints. Thus, modifying the changing aspects of Parkinson's disease. The inter-connection within STN-GPe neurons is robust as seen in Figure 7 and it is evident that they are not involved in recurring movement all the time. Because of the reduction of dopamine, the networks got interrupted among diverse nuclei. But the reason for this dopamine reduction is not so far entirely known. As the stage advances, the effect of medication tends to stop and hinders the quality of life in patients. People at progressive stages of Parkinson's are advised to go for DBS surgery, which can stabilize medicine instabilities, lessen or stop instinctive actions, decrease shake, decrease inflexibility also advance reduction of movement. The activity outlines produced inside STN neuron and input from GPe neuron in a normal state and Parkinson state have been examined in hunt of discovering the parameters which modify the dynamics in Parkinson disorder. For STN-GPe, it has been seen from the result that patterns obtained are effective. Symptoms are reduced up to 99.59%. Here, the cross-correlation coefficient is 0.9959. The maximum coefficient value is 1. The parameters are taken from the previous study profound by me [30, 31].

These studies seek to offer more indication for the usefulness of DBS in the handling of movement disorders, the advantage of early surgery, and the identification of novel goals for formerly treated movement disorders in addition to using 'classic' targets for movement disorders previously untouched by DBS [32]. DBS has infinitely impacted the treatment of

movement disorders, and as it continues to change many more patients may have much to benefit from this treatment modality. In this manuscript, deep brain stimulation has been discussed and the benefits of applying deep brain stimulation in Parkinson's disease person. The values for deep brain stimulation are taken from [11]. Here, deep brain stimulation has been applied mathematically to subthalamic neurons. The results obtained are 99.59% which shows that symptoms are reduced to a great extent. Assessment has been performed for the discharge outlines by examining the compassion in the STN model because of applied current, pre-synaptic membrane potential, feedback synaptic potential, and application of DBS. Both the two-time sequences, i.e., STNHS in regular state and STNPS in Parkinson state, have fewer cross-correlation. When DBS is applied to the STN neuron, it shows maximum cross-correlation. This maximum cross-correlation signifies that the DBS technique is successful for treating patients with Parkinson's disease. Here, one computational model is involved to contemplate in what way DBS of the STN may disturb firing outlines in the basal ganglia model. The next 5 years will be mainly significant for the future of DBS. Numerous multicentre lessons will be concluded and offer vital responses. Indeed, it should be absolutely clear which is the finest target for PD and what alterations there are groups treated with optical medical therapy and with DBS STN [33]. Additionally, while the goal of the surgery is to restore the patient's quality of life, it is also significant to confer safety of indoor and outdoor activities [34].

6. Conclusion:

From the outlines obtained in Fig. 7, it is evident how the Parkinson's disease patterns have come down to normal person's patterns by applying DBS. Therefore, it has been mathematically found out that DBS is a successful treatment for treating patients with Parkinson's disease. The main fact of our outcomes is that DBS may be operative at dropping motor indications of parkinsonism by 99.59%. Consequences recommend that there are further essential parameters that can modify the movement outlined in Parkinson's disease also may progress the changed disorder outlines which are associated with a normal state. The next step of my research is to simulate the parameters which play a vital role in deep brain simulation (DBS).

References:

- [1] Rubin J, McIntyre C, Turner R, Wichmann T. Basal ganglia activity patterns in parkinsonism and computational modeling of their downstream effects. *European Journal of Neuroscience*. 2012;36(2):2213 - 2228. doi: 10.1111/j.1460-9568.2012.08108.x
- [2] Daneshzand M, Faezipour M, Barkana B. Robust desynchronization of parkinson's disease pathological oscillations by frequency modulation of delayed feedback deep brain stimulation. *Plos One*. 2018;13(11):e0207761. doi:10.1371/journal.pone.0207761
- [3] Jiang X, Liu S, Lu B, Zeng Y. High-frequency stimulation for parkinson's disease and effects on pathways in basal ganglia network model. *Journal of Medical and Biological Engineering*. 2016;36(5):704 - 717. doi:10.1007/s40846-016-0170-8
- [4] Anderson D, Beecher G, Ba F. Deep brain stimulation in parkinson's disease: new and emerging targets for refractory motor and nonmotor symptoms. *Parkinson's Disease*. 2017:1-13. doi: 10.1155/2017/5124328

- [5] Williams N, Foote K, Okun M. Subthalamic nucleus versus globus pallidus internus deep brain stimulation: translating the rematch into clinical practice. *Movement Disorders Clinical Practice*. 2014;1(1):24 - 35. doi: 10.1002/mdc3.12004
- [6] Singh J, Singh P, Malik V. Role of sodium, potassium and synaptic conductance in STN-GPe model of basal ganglia in parkinson disease. *Soft Computing Applications*. 2018:81-95. doi: 10.1007/978-981-10-8049-4_4
- [7] Eitan R, Bergman H, Israel Z. Closed-loop deep brain stimulation for parkinson's disease. *Surgery for Parkinson's Disease*. 2018:131-149. doi: 10.3389/fnhum.2021.633655
- [8] Shouno O, Tachibana Y, Nambu A, Doya K. Computational model of recurrent subthalamo-pallidal circuit for generation of parkinsonian oscillations. *Frontiers in Neuroanatomy*. 2017;11(21). doi: 10.3389/fnana.2017.00021
- [9] Pissadaki E, Bolam J. The energy cost of action potential propagation in dopamine neurons: clues to susceptibility in parkinson's disease. *Frontiers in Computational Neuroscience*. 2013;7(13). Doi: 10.3389/fncom.2013.00013
- [10] Maiti P, Manna J, Dunbar G. Current understanding of the molecular mechanisms in parkinson's disease: targets for potential treatments. *Translational Neurodegeneration*. 2017;6(1). Doi: 10.1186/s40035-017-0099-z
- [11] Rubin J, Terman D. High-frequency stimulation of the subthalamic nucleus eliminates pathological thalamic rhythmicity in a computational model. *Journal of Computational Neuroscience*. 2004;16(3):211-235.
- [12] Mostofi A, Evans J, Partington-Smith L, Yu K, Chen C, Silverdale M. Outcomes from deep brain stimulation targeting subthalamic nucleus and caudal zona incerta for parkinson's disease. *npj Parkinson's Disease*. 2019;5(1).
- [13] Singh J, Singh P, Malik V. Effect of intrinsic parameters on dynamics of STN model in parkinson disease: A sensitivity-based study. *Advances in Intelligent Systems and Computing*, 2018:417-427.
- [14] Lanciego J, Luquin N, Obeso J. *Functional neuroanatomy of the basal ganglia*. Cold Spring Harbor. *Perspectives in Medicine*. 2012;2(12):a009621-a009621.
- [15] Singh J, Singh P, Malik V. Sensitivity analysis of discharge patterns of the subthalamic nucleus in the model of basal ganglia in parkinson disease. *Journal of Integrative Neuroscience*. 2018;16(4):441-452.
- [16] Singh J, Singh P, Malik V. Analysis of the firing behavior of STN-GPe network in parkinson disease. *Proceedings of the International Conference on Computing and Communication Systems*. 2018:791-799.
- [17] Navarro-López E, Çelikok U, Şengör N. A dynamical model for the basal ganglia-thalamo-cortical oscillatory activity and its implications in parkinson's disease. *Cognitive Neurodynamics*. 2020;15(4):693-720.
- [18] Martinez-Ramirez D, Hu W, Bona A, Okun M, Shukla A. Update on deep brain stimulation in parkinson's disease. *Translational Neurodegeneration*. 2015;4(1).
- [19] Guo Y, Rubin J, McIntyre C, Vitek J, Terman D. Thalamocortical relay fidelity varies across subthalamic nucleus deep brain stimulation protocols in a data-driven computational model. *Journal of Neurophysiology*. 2008;99(3):1477-1492.
- [20] Gorzelic P, Schiff S, Sinha A. Model-based rational feedback controller design for closed-loop deep brain stimulation of parkinson's disease. *Journal of Neural Engineering*. 2001;10(2):026016.
- [21] Dovzhenok A, Rubchinsky L. On the origin of tremor in parkinson's disease. *PloS One*. 2012;7(7):e41598.

- [22] Gelb D, Oliver E, Gilman S. Diagnostic criteria for parkinson disease. *Archives of Neurology*. 1999;56(1):33.
- [23] Terman D, Rubin J, Yew A, Wilson C. Activity patterns in a model for the subthalamopallidal network of the basal ganglia. *The Journal of Neuroscience*, 2002;22(7):2963-2976.
- [24] Benazzouz A, Piallat B, Ni Z, Koudsie A, Pollak P, Benabid A. Implication of the subthalamic nucleus in the pathophysiology and pathogenesis of parkinson's disease. *Cell Transplantation*. 2000;9(2):215-221.
- [25] Guiyeom K, Lowery M. Conductance-based model of the basal ganglia in parkinson's disease. *IET Irish Signals and Systems Conference (ISSC 2009)*.
- [26] Pascual A, Modolo J, Beuter A. Is a computational model useful to understand the effect of deep brain stimulation in parkinson's disease?. *Journal of Integrative Neuroscience*. 2006;05(04):541-559.
- [27] So R, Kent A, Grill W. Relative contributions of local cell and passing fiber activation and silencing to changes in thalamic fidelity during deep brain stimulation and lesioning: a computational modeling study. *Journal of Computational Neuroscience*. 2011;32(3):499-519.
- [28] De Lau L, Breteler M. Epidemiology of parkinson's disease. *The Lancet Neurology*. 2006;5(6):525-535.
- [29] Feng X, Greenwald B, Rabitz H, Shea-Brown E, Kosut R. Toward closed-loop optimization of deep brain stimulation for parkinson's disease: concepts and lessons from a computational model. *Journal of Neural Engineering*. 2007;4(2):L14-L21.
- [30] Gupta S, Pandey R, Singh J. Study of globus pallidus external and sub thalamic neuron for various currents. *Procedia Computer Science*. 2018;13:1850-1856.
- [31] Gupta S, Singh J, Kumar K. Analyzing and modeling of activity patterns of stn-gp network in parkinson's state vs normal state. *PalArch's Journal of Archaeology of Egypt / Egyptology*. 2020;17(9):9653-9663.
- [32] Kalia SK, Sankar T, Lozano AM. Deep brain stimulation for Parkinson's disease and other movement disorders. *Curr Opin Neurol*. 2013 Aug;26(4):374-80.
- [33] Moro E, Lang AE. Criteria for deep-brain stimulation in Parkinson's disease: review and analysis. *Expert Rev Neurother*. 2006 Nov;6(11):1695-705.
- [34] Machado A, Rezai AR, Kopell BH, Gross RE, Sharan AD, Benabid AL. Deep brain stimulation for Parkinson's disease: surgical technique and perioperative management. *Mov Disord*. 2006 Jun;21 Suppl 14:S247-58.